Journal of Alloys and Compounds 509 (2011) 8912–8916

Contents lists available at ScienceDirect

Journal of Alloys and Compounds

journal homepage: www.elsevier.com/locate/jallcom

Application of statistical methodology for the evaluation of mechanically activated phase transformation in nanocrystalline TiO_2

Masih Rezaee [a,b,*], Seyyed Mohammad Mousavi Khoie [a], Davoud Haghshenas Fatmehsari [a], Hua Kun Liu [b]

[a] Mining and Metallurgical Engineering Department, Amirkbair University of Technology, P.O. Box 15875 4413, Tehran, Iran
[b] Institute for Superconducting and Electronic Materials (ISEM), ARC Centre for Electromaterials Science, University of Wollongong, NSW 2522, Australia

ARTICLE INFO

Article history:
Received 12 May 2011
Received in revised form 30 May 2011
Accepted 3 June 2011
Available online 29 June 2011

Keywords:
Mechanical milling
Polymorphic phase transformation
Rietveld refinement method
TiO_2

ABSTRACT

Response surface methodology was employed to study the effect of three factors, namely as milling time, milling speed and ball to powder weight ratio, on the mechanical activation of polymorphic phase transformation in nanocrystalline TiO_2 powder and identify the probable interactions between these factors. The response was the rutile percentage after annealing the samples. Based on the statistical analysis, ball to powder weight ratio was found as the most effective factor and just one statistically significant interaction was found between milling speed and ball to powder ratio. It was also shown that increasing the milling time has no significant effect on the phase transformation since the required activation energy for the phase transformation is unattainable under these conditions. The rutile percentage was calculated from X-ray diffraction patterns of the samples via Rietveld refinement method. Raman spectroscopy was employed to verify the phase composition analysis based on X-ray diffraction results.

1. Introduction

The polymorphic phase transformation from anatase to rutile in titanium dioxide (TiO_2) has been extensively investigated due to its interests to scientific and engineering fields. The fact that a large number of reports have been published and are still being published indicates its importance [1–6]. Since it is well known that phase composition of TiO_2 is one of the most critical parameters determining its properties in different applications, many researchers have attempted to understand and control the polymorphic phase transformation in this material especially anatase to rutile one [3,7–15]. Even though abundant data have been collected, many issues, such as the effect of particle size and treatment conditions, still remain obscure. The effect of treatment conditions becomes more critical in mechanically processing methods like mechanical milling. In the case of large sized (millimeter-size) single crystals of anatase, it was proposed that rutile nucleates on the surface of the anatase crystallites at the temperature range of 900–950 °C [16]. TiO_2 is a monotropic material and the transformation temperature of anatase to rutile depends on the employed precursor and the particle size, as well as the treatment method [17]. It was reported, however, that the polymorphic phase transformation of TiO_2 can be activated at temperatures as low as ambient temperature via mechanical milling method [4,6,8,18–20]. In spite of this great potential, the characteristics of this method and the accurate effect of its parameters on the transformation have not been completely understood by the researchers because of the limitations for in situ analysis inside the milling jars [21]. The much lower temperature of mechanically activated transformation in comparison with the thermally activated one can be attributed to the presence of the amorphous phase in the former transformation. The crystallization temperature of the amorphous phase to rutile phase is lower than that of anatase to rutile transformation because of the higher driving force of the former transformation [22].

Different factors can affect the polymorphic phase transformation during mechanical milling. However, previous studies on different milling parameters affecting the TiO_2 phase transformation have been conducted by employing the 'one-factor-at-a-time' methodology [1,23–26]. Such a methodology fails to reveal any interactions that may occur amongst the factors [27], whereas these interactions might be important. To the authors' best knowledge, there is no through work reporting the simultaneous effect of milling parameters and their probable interaction on the phase transformation behavior of TiO_2. Recently, soft computing intelligence techniques, such as artificial neural networks (ANN) and genetic algorithms (GA), as well as statistical experiment design techniques, such as response surface method (RSM), have been widely applied in many engineering and research issues. RSM is

* Corresponding author at: Mining and Metallurgical Engineering Department, Amirkbair University of Technology, P.O. Box 15875 4413, Tehran, Iran. Tel.: +98 21 64542949; fax: +98 21 64542941.
E-mail address: m_rezaee@aut.ac.ir (M. Rezaee).

0925-8388/$ – see front matter © 2011 Elsevier B.V. All rights reserved.
doi:10.1016/j.jallcom.2011.06.015

Table 1
Experiments designed by employing central composite design approach.

Run number	Factors			Response (mean ± SD) rutile (wt%)
	t (hour)	V (rpm)	BPR	
1	2	400	10	1.100 ± 1.10
2	2	600	10	3.895 ± 0.06
3	5	400	10	2.620 ± 0.61
4	5	600	10	7.915 ± 0.69
5	2	400	30	48.280 ± 0.40
6	2	600	30	94.635 ± 2.91
7	5	400	30	70.110 ± 0.09
8	5	600	30	93.225 ± 6.78
9	3.5	400	20	25.020 ± 3.09
10	3.5	600	20	83.170 ± 3.46
11	2	500	20	58.050 ± 3.98
12	5	500	20	94.345 ± 3.07
13	3.5	500	10	3.985 ± 0.15
14	3.5	500	30	81.030 ± 2.30
15	3.5	500	20	60.485 ± 7.74
16	3.5	500	20	80.175 ± 0.66
17	3.5	500	20	80.600 ± 5.88
18	3.5	500	20	73.855 ± 3.14

one of the most powerful collections of mathematical and statistical design tools which is able to simultaneously consider several factors at different levels and give a model for the correlation between the various factors and the response. In these applications, the engineering objective is to find the significant variables together with their optimum values, and the possible interactions between each two effective factors. RSM has been applied in a wide variety of industrial setting and parameter optimizations such as chemical, semiconductor and electronic manufacturing, machining, and metal cutting processes. Not only it can save a lot of time but also can build models quickly and accurately in an optimization design [28].

The present work addresses a fairly complete investigation of the effect of milling parameters on TiO_2 polymorphic phase transformation with the help of response surface methodology using a central composite design (CCD). The relative content of different phases in the samples was calculated via Rietveld refinement of X-ray diffraction patterns and confirmed via Raman spectroscopy.

2. Materials and methods

2.1. Ball milling experiments

Fully anatase phase nanocrystalline TiO_2 powder (Sigma–Aldrich) with mean crystallite size of around 70 nm was used as the starting material of milling experiments. Eighteen milling runs with two replicates for each one was designed applying response surface methodology. Milling was conducted in a high-energy planetary ball mill consisting of two hard chromated stainless steel jars. A 70:30 ratio (weight percent) mixture of 10–5 mm in diameter hard chromated stainless steel balls was used during milling process. Each jar was loaded with five-gram powder. As-milled samples were annealed at 850 °C for 2 h to promote the TiO_2 phase transformation to be completed.

2.2. Design of experiment via response surface methodology

Eighteen runs consisting of 6 star points (star distance was 0) and 4 center points were generated by the principle of RSM using MINITAB Release 15. To develop a second order polynomial model, a central composite design (CCD) with multiple linear regression was employed to estimate the model coefficients of the three selected factors believed to influence rutile content of the samples, with each factor set at its high level (+1), low level (−1) and medium level (0).

Amongst different milling parameters, milling speed, milling time and ball to powder weight ratio were selected to be investigated due to their higher importance reported in literature [4,6,25,29,30]. Experiments were conducted at different levels of the factors based on the previous works [1,6,7,18,23,29–31]. The levels used for these three factors, according to a CCD, are listed in Table 1. The post-annealing parameters for all experiments were kept constant to provide appropriate conditions to evaluate the effect of the mechanical milling on the activation of polymorphic phase transformation of nanocrystalline TiO_2 powder at ambient temperature.

All the experiments were performed with two replicates and the results for the response were reported as a mean value of each two responses in a randomized order to avoid systematic bias.

Finally, a quadratic polynomial regression model (Eq. (1)) was employed to estimate and predict the response value over a range of input factors' values [27]:

$$Y = b_0 + \sum_{i=1}^{k} b_i X_i + \sum_{i=1}^{k} b_{ii} X_i^2 + \sum_{i=1}^{k-1} \sum_{j=i+1}^{k} b_{ij} X_i X_j \quad (1)$$

where Y is the dependant response variable (i.e. the percentage of rutile phase in milled powders after annealing for 2 h at 850 °C), b_0 is the intercept term, b_i, b_{ii}, and b_{ij} are the measures of the effect of variable X_i, $X_i{}^2$ and X_iX_j, respectively. X_i and X_j represent the independent variables and k is the number of these factors. In this case k is three and includes milling time (t), milling speed (V) and ball to powder weight ratio (BPR). The variable X_iX_j represents the first order interaction between X_i and X_j ($i < j$). The purposes of considering a model such as (Eq. (1)) are [32]:

1. To establish a relationship, albeit approximate, between y and $X_1, X_2, \ldots, X_k$ that can be used to predict response value (Y) for a given settings of the control variables.
2. To determine, through hypothesis testing, significance of the factors whose levels are represented by $X_1, X_2, \ldots, X_k$.
3. To estimate the optimum settings of $X_1, X_2, \ldots, X_k$ that result in the maximum (or minimum) response over a certain region of interest.

The analysis of variance (ANOVA) for quadratic model was performed at 10% confidence level (P-value < 0.1). The significance and the magnitude of the effects estimations for each variable and all their possible linear and quadratic interactions were also determined. At last, the model was used to predict main effective factors. All the analysis was carried out using MINITAB Release 15.

2.3. Characterization methods

Phase characterization of the powders was conducted using a GBC MMA X-ray diffractometer (XRD) with Cu Kα_1 radiation (λ = 1.54056 Å) in the 2θ range of 20–100° with a step size of 0.02° and a step time of 1.2 s. The dependant response variable of the design of experiment (rutile percentage) was calculated via Rietveld powder structure refinement method employing Materials Analysis Using Diffraction (MAUD) software (Version 2.26) [33]. Popa fitting model [34] was utilized to analyze the XRD patterns. The crystallographic information as well as starting parameters of site occupancies and lattice parameters were taken from database of the analyzing Rietveld program (MAUD).

In order to confirm the values calculated from XRD patterns for the relative phase contents, three samples were selected to be investigated via Raman spectroscopy method. The samples were chosen in such a way to have different compositions as one fully anatase phase (sample 1), one fully rutile phase (sample 8) and one with a combination of anatase and rutile phases (sample 7). Raman spectra were collected employing a confocal Raman microscope of LabRAM HR, Horiba Jobin Yvon SAS.

3. Results and discussion

3.1. Calculation of the response

The overlaid XRD patterns of all eighteen samples are shown in Fig. 1. As it can be seen, XRD patterns of all samples include different peaks related to both anatase and rutile phases with different intensity ratios. In order to determine the relative content of individual polymorphic TiO_2 phases in all samples, a full pattern modeling method, named Rietveld refinement method [33], was employed to fit the experimental XRD patterns with the theoretical patterns drawn according to the existing crystallographic data by the use of MAUD software. This methodology takes care of all reflections stemmed from each phase present in such a multiphase material, whether overlapped or not, and provide a very accurate result. Close observation of Fig. 1 reveals that different levels of milling factors can result in various phase compositions ranged from a fully anatase phase to a fully rutile phase. The ability of milling processing method to drive a phase transformation through different ways seems to be an appropriate and helpful alternative where different phase compositions are required for achieving a variety range of properties.

Fig. 2 shows the Raman spectra of three selected samples (1, 7 and 8) recorded with a laser beam of 632.8 nm wavelength. Anatase

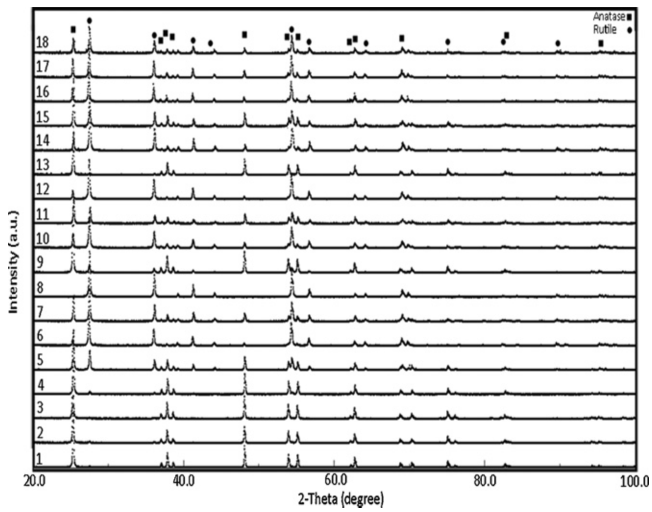

Fig. 1. XRD patterns of all eighteen samples prepared based on experimental design.

is tetragonal and belongs to the space group $I4/amd$ [35]. There are six allowed bands in the first-order Raman spectrum of anatase at 144 cm^{-1} (E_g), 197 cm^{-1} (E_g), 399 cm^{-1} (B_{1g}), 516 cm^{-1} ($A_{1g}+B_{1g}$), and 639 cm^{-1} (E_g). The Raman band occurring at 516 cm^{-1} at ambient temperature is split into two peaks centered at 513 cm^{-1} (A_{1g}) and 519 cm^{-1} (B_{1g}) at 73 K [2]. Rutile is also tetragonal and belongs to the space group $P4_2/mnm$ [35]. There are four Raman active modes with symmetry of A_{1g}, B_{1g}, B_{2g}, and E_g at 143 cm^{-1} (B_{1g}), 447 cm^{-1} (E_g), 612 cm^{-1} (A_{1g}), and 826 cm^{-1} (B_{2g}) [2]. As it can be seen in Raman spectra of samples 1, 7 and 8 (Fig. 2), the Raman bands located at ∼138 cm^{-1}, ∼192 cm^{-1}, ∼393 cm^{-1}, ∼515 cm^{-1}, and ∼636 cm^{-1} can be ascribed to the anatase phase, and the bands located at ∼138 cm^{-1}, ∼237/242 cm^{-1}, ∼439 cm^{-1}, and ∼617 cm^{-1} can be assigned to the rutile phase. Regarding the intensity and the width of the Raman bands of these three samples, it is very likely for sample 1 to be completely consisted of anatase, which is in conformity with the result of XRD calculations (1.10%). The second-order scattering is more intense than one-phonon scattering in rutile, while in the case of anatase, only a few weak bands are observed due to two-phonon scattering [2,36]. Furthermore, for the samples containing both anatase and rutile such as sample 7, a small hint of some weak Raman bands appears in the shoulder of the rutile's

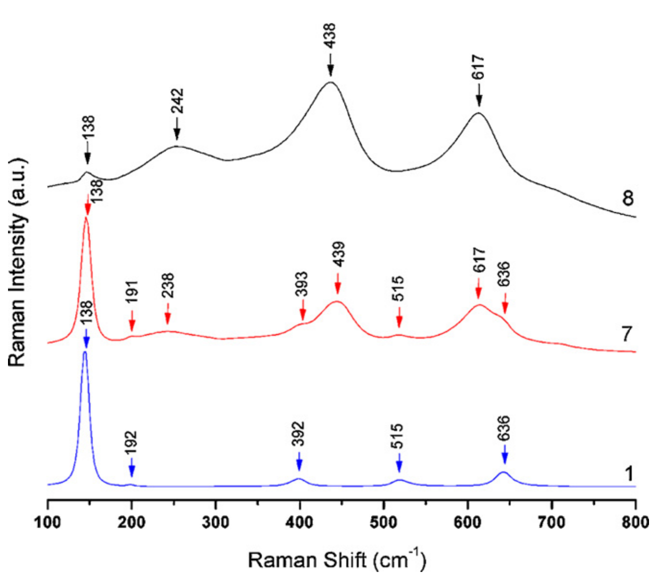

Fig. 2. Raman spectra of samples 1, 7 and 8.

Table 2
Values of regression coefficients calculated for the rutile percentage after annealing the milled samples for 2 h at 850 °C.

Independent factor	Regression coefficient	Standard error	T-value	P-value
Constant	−474.549	168.718	−2.813	0.023
Linear				
t	−21.094	26.513	−0.796	0.449
V	1.667	0.717	2.327	0.048
BPR	9.115	3.632	2.510	0.036
Quadratic				
$t{\cdot}t$	4.090	3.131	1.306	0.228
$V{\cdot}V$	−0.014	0.001	−2.333	0.048
BPR·BPR	−0.246	0.070	−3.498	0.008
Interactive				
$t{\cdot}V$	−0.014	0.027	−0.498	0.632
t·BPR	0.162	0.273	0.592	0.570
V·BPR	0.008	0.008	1.848	0.102

Raman bands at high wave numbers (Fig. 2) which can be attributed to the anatase phase. Such a conclusion for sample 7 is in a well semi-quantitative agreement with XRD calculations (∼70% rutile). All the Raman bands in the Raman pattern of sample 8 (Fig. 2) are consistent with Raman bands related to rutile phase. XRD calculations also show that this sample almost completely consists of rutile phase with a small hint of anatase phase.

3.2. Model fitting

The values of rutile percentage of the milled samples after annealing for 2 h at 850 °C are listed in Table 1 for all 18 combinations of factor levels. It can be observed that these values cover a complete range of transformation from anatase to rutile from around 0 to 100% which is an evidence for the appropriate selection of the factors' levels.

Table 2 presents the values of the regression coefficients. At 10% confidence level, two linear terms of V and BPR, quadratic terms of V and BPR as well as interactive term of $V \times$ BPR are statistically significant. According to the results presented in Table 2, the effect of milling time (t) on mechanical activation of polymorphic phase transformation in nanocrystalline TiO_2 powder is statistically insignificant; in other words, the amount of rutile in mechanical activation process of phase transformation is independent of the milling time. If the impact energy attained by the particles is lower than the required energy for activating the polymorphic phase transformation, increasing the milling time cannot promote the transformation process [37]. On the other hand, according to the results of Table 2, both milling speed (V) and ball to powder weight ratio (BPR) play the major roles in providing the required transformation energy in which, size of balls should be selected in such a way that can provide sufficient energy to activate the phase transformation. Afterwards, at high levels (+1) of these two parameters, an increase in milling time can promote the polymorphic phase transformation in nanocrystalline TiO_2 powder.

According to the calculated values for the regression coefficients (Table 2), a polynomial equation is proposed as follows:

$$\text{Rutile\%} = -474.549 + 10667\ (V) + 9.115\,(\text{BPR}) - 0.002\,(V)^2 - 0.246\,(\text{BPR})^2 + 0.008(V \cdot BPR) \qquad (2)$$

This equation fits 93.64% with the variations in data. As it was mentioned above, milling time (t) and speed (V) and BPR are the independent factors of experimental design, while the rutile percentage is the dependent parameter of the process. The concept of ANOVA is really quite simple: to compare different sources of variance and make inferences about their relative sizes [38]. It is fundamental that an experiment is designed properly for the data

Table 3
ANOVA table.

	Df[a]	SS[b]	MS[c]	F-values	P-values
Total	17	21061.4			
Regression	5	19322.8	3864.57	26.68	0.000
Residual error	12	1738.5	144.88		
Lack of fit (model error)	3	840.1	280.02	2.81	0.101
Pure error (Replicate error)	9	898.4	99.83		
R^2	94.89%				

[a] Df = degrees of freedom.
[b] SS = sum of squares.
[c] MS = mean squares.

to be useful and reliable. ANOVA is a useful system to check the main influence of a factor and the contribution due to its interaction with the others. ANOVA results of milling activation of polymorphic phase transformation in nanocrystalline TiO_2 powder are listed in Table 3. The estimated *P*-value for the regression ($P \leq 0.1$) together with this value for the lack of fit ($P > 0.1$), indicate the suitability of the model.

3.3. Study of mainly effective factors

In order to investigate the most effective factor in mechanical activation of polymorphic phase transformation in nanocrystalline TiO_2 powder, the main effects plots for rutile percentage were plotted (Fig. 3).

The plots demonstrate that how different factors affect the independent response (rutile percentage). As it can be seen from Fig. 3, response variation is around 80% by changing BPR from its lowest level to the highest one; while this variation is around 35% for milling speed under the same change in the level of *V*. Thus, BPR is the most significant factor amongst three factors in the studied ranges.

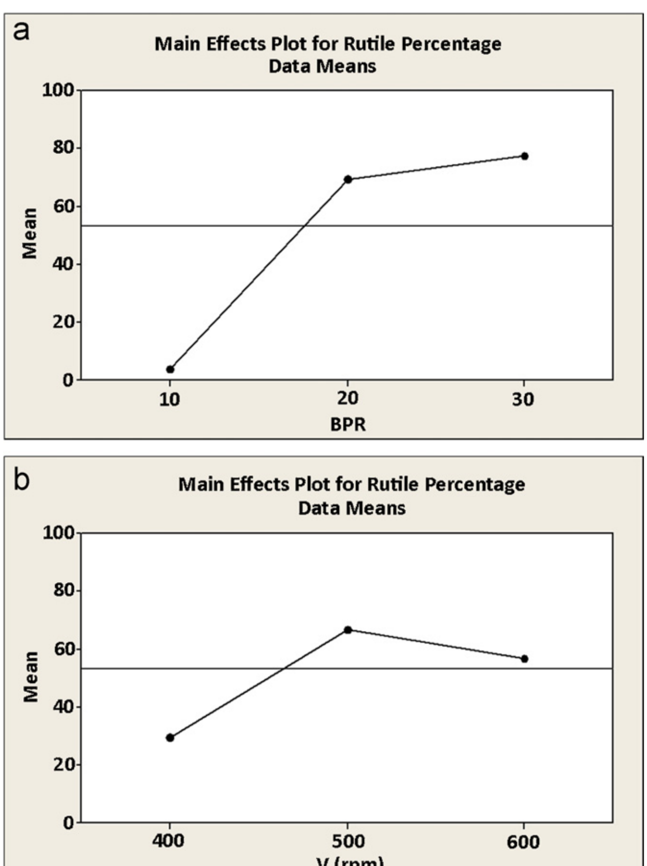

Fig. 3. Main effects plots for rutile percentage.

The effect of the ball to powder weight ratio (BPR) (Fig. 3(a)) can be explained based on the fact that the required time for the completion of mechanically activated transformation decreases with an increase in BPR due to the higher collision energy at higher BPRs [21]. In contrast, the main effect plot of milling speed (*V*) (Fig. 3(b)) shows an optimum value for the response. It is very likely that the faster the mill rotates, the higher would be the energy gained by the powder. However, above a critical speed, the balls are pinned onto the inner walls of the jar and, hereby, do not fall down to exert any impact force. Consequently, the maximum speed should be just below a critical value so that the balls fall down from the maximum height to generate the maximum collision energy [21]. The only remained point is the time of milling. Although milling time is an insignificant factor in the studied range, it should be essentially so chosen as to achieve a steadiness between the fracturing and cold welding of the powder particles to prevent high agglomeration in very long times. Agglomeration can act as a barrier for further transformation. Consequently, it is better to mill the powder just for the required duration and not any longer. On the other hand, it should be noted that increasing the milling time wastes more energy and enhances the probability of contamination [21].

3.4. Study of interaction amongst milling factors

In the cases where interaction between two factors is statistically significant, surface plots give more complete information regarding the effect of a factor on the response. Surface plot presented in Fig. 4 shows the mutual effect of the *V* and BPR factors on the rutile weight percentage of the milled samples after annealing for 2 h at 850 °C.

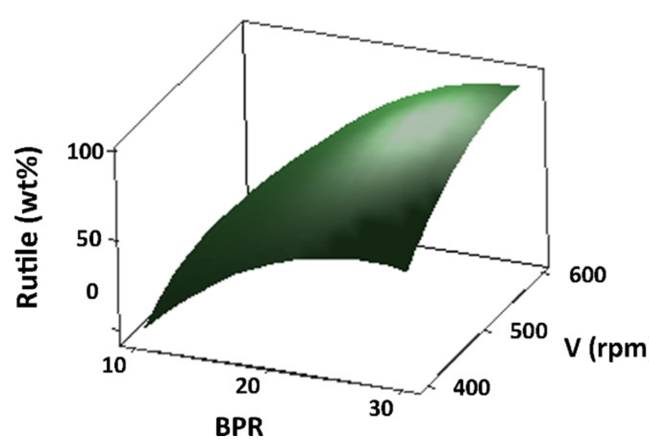

Fig. 4. Surface plot for rutile weight percentage of milled samples after annealing for 2 h at 850 °C with respect to *V* and BPR (with milling time fixed at its middle value).

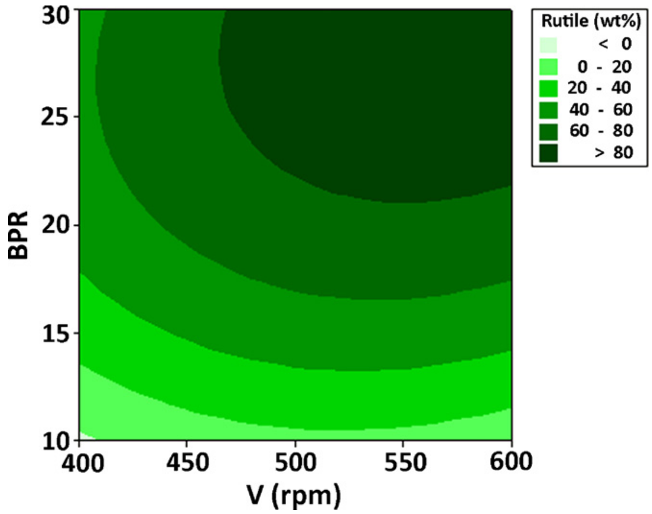

Fig. 5. Contour plot for rutile weight percentage of milled samples after annealing for 2 h at 850 °C with respect to *V* and BPR (with milling time fixed at its middle value).

As it can be seen in Fig. 5, the effect of milling speed (*V*) becomes more crystallized in mechanically activated phase transformation of nanocrystalline TiO_2 with increasing BPR. Such a trend can be observed when both BPR and *V* increase. Since the charge weight of the initial powders is constant for all the experiments, the balls number increases with an increase in BPR. Consequently, the powders participated in each collision decreases by increasing BPR [7]. Considering two different experiments with the same milling speed, it can be concluded that for a given collision time, an increase in BPR leads to higher energy releasing for each particle. On one hand, the collision frequencies of both ball to ball and ball to wall impacts increase by increasing *V* which in turn, leads to a higher kinetics energy transfer to the particles. The higher kinetics energy results in an excessive microstructural defects such as dislocations and vacancies [39]. On the other hand, it is very likely that the microstructural changes in higher milling speeds reduce the microstructural diffusion path lengths. Since "nucleation and growth" mechanism is the predominant mechanism on mechanically activated phase transformation in nanocrystalline TiO_2 [6], the presence of microstructural defects as well as shortening the diffusion paths can promote the phase transformation rate. Additionally, the higher impact energy due to an increase in both *V* and BPR factors may potentially provide the sufficient energy for the activation of phase transformation. As a result, it seems that the simultaneous increase of these two factors has a synergistic effect on the phase transformation rate promotion.

Fig. 5 shows the contour plot for rutile weight percentage with respect to *V* and BPR factors. As it can be seen in this plot, the changing range of BPR factor becomes limited to its higher values with increasing *V* factor to its higher values and vice versa. Such a trend in contour plot also proves the synergistic effect of *V* and BPR on the phase transformation rate.

4. Conclusion

Response surface methodology was employed to investigate the mechanical activation of the polymorphic phase transformation in nanocrystalline TiO_2 powder and to examine the effect of three most effective factors namely as milling time, speed and ball to powder weight ratio on it. Just one statistically significant interaction was found between milling speed and ball to powder weight ratio. It was shown that the milling time can be a statistically insignificant factor on the phase transformation unless the required energy for the activation of phase transformation is provided by proper selection of the other factors' levels. It was also found that the effect of ball to powder weight ratio on polymorphic phase transformation in nanocrystalline TiO_2 is much higher than milling speed's effect. It was observed that the higher ball to powder weight ratio, the more rutile phase in the milled powder after annealing. There is an optimum value for milling speed in which the rutile percentage approaches to its maximum value. A fairly good agreement between XRD and Raman spectroscopy results was found regarding the phase composition of the powder samples.

References

[1] P. Bose, S.K. Pradhan, S. Sen, Materials Chemistry and Physics 80 (2003) 73–81.
[2] C. Chen, Y. Huang, W. Chung, D. Tsai, K. Tiong, Journal of Materials Science: Materials in Electronics 20 (2009) 303–306.
[3] I.L. Cooper, T.A. Egerton, F. Qiu, Journal of the European Ceramic Society 29 (2009) 637–646.
[4] X. Pan, Y. Chen, X. Ma, L. Zhu, Journal of the American Ceramic Society 87 (2004) 1164–1166.
[5] X. Pan, X. Ma, Journal of Solid State Chemistry 177 (2004) 4098–4103.
[6] M. Rezaee, S.M. Mousavi Khoie, Journal of Alloys and Compounds 507 (2010) 484–488.
[7] S. Bégin-Colin, T. Girot, G. Le Caër, A. Mocellin, Journal of Solid State Chemistry 149 (2000) 41–48.
[8] H.-I. Hsiang, S.-C. Lin, Ceramics International 34 (2008) 557–561.
[9] J.P. Xu, S.B. Shi, L. Li, J.F. Wang, L.Y. Lv, F.M. Zhang, Y.W. Du, Journal of Physics and Chemistry of Solids 70 (2009) 511–515.
[10] Y. Shao, D. Tang, J. Sun, Y. Lee, W. Xiong, China Particuology 2 (2004) 119–123.
[11] D.J. Reidy, J.D. Holmes, M.A. Morris, Journal of the European Ceramic Society 26 (2006) 1527–1534.
[12] A. Ogden, J.A. Corno, J.-I. Hong, A. Fedorov, J.L. Gole, Journal of Physics and Chemistry of Solids 69 (2008) 2898–2906.
[13] B.J.M.A.N. Giridhar Madras, Journal of the American Ceramic Society 90 (2007) 250–255.
[14] C. Suresh, V. Biju, P. Mukundan, K.G.K. Warrier, Polyhedron 17 (1998) 3131–3135.
[15] Y. Djaoued, S. Badilescu, P.V. Ashrit, D. Bersani, P.P. Lottici, J. Robichaud, Journal of Sol–Gel Science and Technology 24 (2002) 255–264.
[16] R.D. Shannon, J.A. Pask, American Mineralogist 49 (1964) 1707–1718.
[17] L.J. Alemany, M.A. Baoares, E. Pardo, F. Martin-Jiménez, J.M. Blasco, Materials Characterization 44 (2000) 271–275.
[18] F. Delogu, Journal of Alloys and Compounds 468 (2009) 22–27.
[19] L. Gonzalez-Reyes, I. Hernandez-Pérez, F.C. Robles Hernandez, H.D. Rosales, E.M. Arce-Estrada, Journal of the European Ceramic Society 28 (2008) 1585–1594.
[20] E. Napolitano, G. Mulas, S. Enzo, F. Delogu, Acta Materialia 58 (2010) 3798–3804.
[21] C. Suryanarayana, Progress in Materials Science 46 (2001) 1–184.
[22] R. Ren, Z. Yang, L.L. Shaw, Journal of Materials Science 35 (2000) 6015–6026.
[23] E. Arca, G. Mulas, F. Delogu, J. Rodriguez-Ruiz, S. Palmas, Journal of Alloys and Compounds 477 (2009) 583–587.
[24] H. Dutta, Y.C. Lee, S.K. Pradhan, Physica E: Low-dimensional Systems and Nanostructures 36 (2007) 17–27.
[25] N. Setoudeh, A. Saidi, A. Shafyei, N.J. Welham, Esteghlal 25 (2006) 207–216.
[26] M. Uzunova-Bujnova, D. Dimitrov, D. Radev, A. Bojinova, D. Todorovsky, Materials Chemistry and Physics 110 (2008) 291–298.
[27] D.C Montgomery, Design and Analysis of Experiments, 6th ed., John Wiley & Sons, New York, 2006.
[28] T.-H. Hou, C.-H. Su, W.-L. Liu, Powder Technology 173 (2007) 153–162.
[29] M. Salari, S.M. Mousavi khoie, P. Marashi, M. Rezaee, Journal of Alloys and Compounds 469 (2009) 386–390.
[30] M. Salari, M. Rezaee, S.M. Mousavi Koie, P. Marashi, H. Aboutalebi, International Journal of Modern Physics B 22 (2008) 2955–2961.
[31] M. Rezaee, S.M. Mousavi Khoie, K.H. Liu, CrystEngComm (2011).
[32] A.I. Khuri, S. Mukhopadhyay, Wiley Interdisciplinary Reviews: Computational Statistics 2 (2010) 128–149.
[33] L. Lutterotti, Maud – Materials Analysis Using Diffraction (2010) (New version: 2.26).
[34] N.C. Popa, D. Balzar, Journal of Applied Crystallography 41 (2008) 615–627.
[35] J. Muscat, V. Swamy, N.M. Harrison, Physical Review B 65 (2002) 224112.
[36] M. Salari, S.H. Aboutalebi, K. Konstantinov, H.K. Liu, Physical Chemistry Chemical Physics 13 (2011) 5038–5041.
[37] F. Liu, F. Sommer, C. Bos, E.J. Mittemeijer, International Materials Reviews 52 (2007) 193–212.
[38] P.M. Congedo, A. Ficarella, D. Laforgia, Journal of Heat Transfer 126 (2004) 365–375.
[39] K. Gheisari, S. Javadpour, J.T. Oh, M. Ghaffari, Journal of Alloys and Compounds 472 (2009) 416–420.